Pharm Res (2015) 32:1017–1027
DOI 10.1007/s11095-014-1513-1

RESEARCH PAPER

The Glucose-Lowering Potential of Exenatide Delivered Orally via Goblet Cell- Targeting Nanoparticles

Xiang Li • Chenhui Wang • Rongcai Liang • Fengying Sun • Yanan Shi • Aiping Wang • Wanhui Liu • Kaoxiang Sun • Youxin Li

Received: 5 March 2014 / Accepted: 3 September 2014 / Published online: 1 October 2014

ABSTRACT

Purpose Exenatide, a potent insulinotropic agent, can be used for the treatment of non-insulin-dependent diabetes mellitus. However, the need for frequent injections seriously limits its therapeutic utility. The aim of present report was to develop an orally available exenatide formulation using goblet cell-targeting nanoparticles (NPs).

Method The exenatide-loaded nanoparticles were prepared with modified chitosan which was conjugated with a goblet cell-target peptide, CSKSSDYQC (CSK) peptide.

Results The CSK-chitosan nanoparticles shown reduced chitosan toxicity and enhanced the permeation of drugs across the Caco-2/HT-29 co-cultured cell monolayer, which simulated the intestinal epithelium. Following the oral administration of near-infrared fluorescent probe Cy-7-loaded NPs to mice, the distribution of the drugs was investigated with a near-infrared *in vivo* image system (FX Pro, Bruker, USA). The results showed that Cy-7 fluorescence disseminated from the oesophagus, then to stomach and small intestine and then was absorbed into hepatic, finally into the bladder; over time, Cy-7 was metabolized and excreted. The bioavailability of the modified nanoparticles was found to be 1.7-fold higher compared with the unmodified ones, and the hypoglycemic effect was also better.

Conclusion CSK peptide-modified chitosan nanoparticles could be a potential therapeutics for Type II diabetes patients.

X. Li • C. Wang • R. Liang • F. Sun • Y. Shi • Y. Li
School of Life Sciences, Jilin University, Changchun 130012, China

X. Li • R. Liang • Y. Shi • A. Wang • W. Liu • K. Sun • Y. Li
State Key Laboratory of Long-acting & Targeting Drug Delivery System
No. 9 Baoyuan Road, 264003 Yantai, Shandong Province, China

R. Liang • A. Wang • W. Liu • K. Sun • Y. Li (✉)
School of Pharmacy, Yantai University
No. 30 Qingquan Road, Yantai, China
e-mail: liyouxin@jlu.edu.cn

KEY WORDS CSK peptide-modified chitosan · exenatide · goblet cell-targeting nanoparticles · *in vivo* image system · oral delivery system

INTRODUCTION

Exendin-4 is an incretin analog that is found in lizard saliva and belongs to a new class of anti-diabetic drugs. Exenatide is a synthetic version of exendin-4, which mimics several glycoregulatory activities of the mammalian hormone glucagon-like peptide-1 (1). In clinical trials, exenatide exhibited glucose regulatory effects, including the stimulation of insulin secretion, according to the blood glucose concentration; the inhibition of inadequately elevated glucagon secretion; and suppression of gastric emptying (2,3). To date, the only route of exenatide administration has been subcutaneous injection, which requires frequent administration and can be painful. Clearly, new administration routes should be investigated.

The oral route of administration is generally considered the most straightforward and comfortable method of drug administration (4). Thus, the oral delivery of exenatide would be advantageous to diabetic patients because it would alleviate the suffering that results from injections. Furthermore, it can mimic the physiological release characteristics of insulin and may show improvements with respect to glucose homeostasis. Nanoparticle is a promising way for peptide orally delivery which can offer drug protection and facilitate drug absorption through the intestinal mucosa. However, developing an efficient nanoparticle for oral delivery is a great challenge as intestinal epithelial cells and mucus layer is the absorption barrier (5).

Chitosan in the form of nanoparticles or nanocapsules has already been used to improve transport across different mucosal surfaces (6,7). Chitosan adheres well to the mucus coat of epithelial tissues because of its ability to induce ephemeral opening of the tight junctions between adjacent cells (8). In addition, there have been no reports of inflammatory or

allergic reactions when using chitosan-based biomaterials in implantation, injection or topical application in the human body (9). Because chitosan is soluble in aqueous acidic solution, the use of hazardous organic solvents is avoided when fabricating the particles (10). Different methods have been employed to prepare chitosan particle systems, including emulsion cross-linking, coacervation/precipitation, spray-drying, emulsion-droplet coalescence, the reverse micellar method, sieving and ionic gelation (9). Because the ionic gelation method is simple and mild, it has attracted much more attention than other methods. For example, tripolyphosphate (TPP), which is a type of polyanion, can electrostatically interact with cationic chitosan (11). Kiran Sonaje *et al.* used poly-(g-glutamic acid) as a polyanion and obtained stable nanoparticles (8).

There are certain types of specific ligands that can target receptors on the surface of epithelial cells. Thus, modified nanoparticles or nanocapsules with these specific ligands can facilitate the oral absorption of peptides and proteins (12). An important step is the exploitation of more effective targeting ligands that provide sufficient targeting effectiveness and are not blocked by mucus (5). Recently, a CSKSSDYQC (CSK) peptide demonstrated affinity for goblet cells, an important component of intestinal epithelial cells. The CSK peptide was identified from a random phage-peptide library using an *in vivo* phage display technique to identify peptides that facilitate the transport of M13 bacteriophages across the intestinal epithelium (13). Yun Jin *et al.* used the CSK peptide to modify trimethyl chitosan chloride and observed an improved hypoglycemic effect, with a 1.5-fold higher relative bioavailability compared with unmodified versions (5).

In this study, we established goblet cell-targeting chitosan nanoparticles using the CSK peptide (CSK-chitosan) to encapsulate exenatide and evaluated their effectiveness as oral exenatide vehicles. The characteristics of the chitosan and CSK-chitosan NPs were examined using a Zeta Potential/Particle Sizer and transmission electron microscopy (TEM). The influence of mucus and the targeting effect *in vitro* were investigated by co-incubation in a Caco-2 and HT29 cell model. The biodistribution of Cy-7-loaded NPs after oral administration in mice was investigated with a near-infrared *in vivo* imaging system. Finally, the relative bioavailability and hypoglycemic effect of the modified targeting NPs were tested in Sprague Dawley (SD) rats and diabetic mice, respectively.

MATERIALS AND METHODS

Materials

Chitosan (deacetylation degree, >90% and molecular weight, 80–100 kDa) was purchased from Qingdao Yunzhou Biochemistry Co., Ltd. (Shandong, China). Exenatide was purchased from Soho-Yiming Pharmaceuticals Co., Ltd. (Shanghai, China). The CSK peptide was chemically synthesized by Qiangyao Bio-pharmaceuticals Co., Ltd. (Shanghai, China). FITC-exenatide was chemically synthesized by GL Biochem (Shanghai) Ltd. (Shanghai, China). 3-(4, 5-Dimethyl-thiazol-2-yl)-2,5-diphenyltetrazolium bromide (MTT) was purchased from Sigma-Aldrich (St. Louis, MO, USA). Cy7 was a product of Fanbo Biochemicals (Beijing, China). Tripolyphosphate (TPP) was purchased from Sigma-Aldrich (St. Louis, MO, USA). All other reagents were analytical grade.

The Caco-2 and HT29 cell lines were purchased from Yantai Yuansheng Biochemistry Co., Ltd. (Shandong, China) and cultured in Dulbecco's Modified Eagle Medium (DMEM) (Gibco, Grand Island, NY, USA) containing 15% fetal calf serum and 1% non-essential amino acids (Gibco).

Animals

Male SD rats weighing approximately 250 g were and the supplied by the State Key Laboratory of Long-acting & Targeting Drug Delivery System. The db/db diabetic mice were purchased from Model Animal Research Center of Nanjing University. The animals were raised at room temperature, approximately 23°C, with a relative humidity of 30± 5%.

Synthesis of CSK-Chitosan

Chitosan was conjugated to the CSK peptide via an amide bond formed between the residual primary amino groups on chitosan and the carboxyl groups on the CSK peptide. Briefly, the CSK peptide was dissolved in PBS (pH 7.2) and kept in a 0°C ice-water bath for at least 15 min. Excess 1-[3-(dimethylamino) propyl]-3-ethylcarbodiimide hydrochloride) (EDC) and N-hydroxysuccinimide (NHS) were added to the CSK peptide solution and allowed to react for 1 h at 0°C ice-water bath with magnetic stirring. The same amount or twice the amount of chitosan was added and allowed to react for 1 h at ambient temperature with magnetic stirring. Subsequently, the product was dialyzed with PBS (pH 7.4), lyophilized and stored at 0°C. The two different CSK peptide-modified chitosan molecules are referred to as CSK-chitosan (1:1) and CSK-chitosan (1:2) (5).

Preparation of NPs

Exenatide-Loaded NPs

The nanoparticles were prepared using the ionotropic gelation method (5). Briefly, exenatide was dissolved in distilled water (2 mg/ml) and added to a chitosan solution (1 mg/ml, containing 0.005%*w*/*v* $FeSO_2$) or a modified CSK-chitosan

solution (1 mg/ml, containing 0.0025%*w/v* $FeSO_2$). Then, a 2.5 mg/ml or 0.625 mg/ml tripolyphosphate (TPP) solution was added dropwise to the chitosan solution or CSK-chitosan solution at a ratio of 3.75:10 or 1:10, respectively, with magnetic stirring. Afterward, the obtained solution was stirred at 500 rpm for 40 min until an opalescent suspension with an obvious Tyndall phenomenon was obtained. The obtained suspension was centrifuged at 3,500 rpm for 25 min at 20°C. The supernatant was used to determine the entrapment efficiency and then lyophilized with 5% sucrose as a cryoprotectant. The FITC-exenatide NPs were made by similar method.

Cy-7-Loaded NPs

For *in vivo* fluorescence imaging, the near-infrared fluorescent probe Cy-7 was loaded into the NPs. The method was similar to that used for exenatide. The NP suspension was eluted using a Sephadex G-50 column to remove free Cy-7.

Characterization of NPs

Size and Zeta Potential

The size and zeta potential of the drug-loaded nanoparticles were characterized with a Zeta Potential/Particle Sizer (NICOMP TM 380ZLS, NICOMP). All measurements were performed six times.

The Morphology of NPs

The NP morphology was examined by TEM (JEM—1400, JEOL, Japan). Briefly, the nanoparticle suspension was added dropwise to 300-mesh copper grids. When the liquid volatized naturally, a drop of 3% phosphotungstic acid was added. After the liquid was volatized, the sample was scanned by TEM.

Encapsulation Efficiency of Exenatide-Loaded NPs

The amount of encapsulated exenatide was measured with a Sephadex G50 gel column. Briefly, a 4-cm gel column was obtained using a 5-ml syringe with a small piece of filter paper blocking the openings. Sephadex G50 was pre-swollen with boiled distilled water. The nanoparticles and free exenatide have different retention times; the nanoparticles elute faster because of their larger size. The eluted nanoparticles were damaged by the addition of acetic acid. The amount of exenatide in the nanoparticles was measured by reverse-phase high-performance liquid chromatography (HPLC) (Agilent 1260 series, CA, USA) using an analytical column (Ultimate® LP-C18, 4.6 mm×250 mm, pore size 5 μm, Agilent) and a gradient elution of (A) acetonitrile containing 5% phosphoric acid and (B) water containing 5% phosphoric acid as the mobile phase. The method utilized was 0 min (30% A)→10 min (44% A)→10.1 min (30% A)→15 min (30% A). The flow rate was set at 1 ml/min, and the elution temperature was 40°C. The retention time of exenatide was 9.5 min, and the total run time for the HPLC analysis was 15.0 min. The amount of FITC-exenatide was also measured by reverse-phase HPLC (Agilent 1260 series) using a fluorescence detector. And the excitation and emission wavelengths were set at 488 and 525 nm, respectively (5,14).

The encapsulation efficiency (EE %) of the exenatide-loaded NPs was calculated using formula I:

$$EE\% = \frac{encapsulated\ exenatide}{total\ amount\ of\ exenatide} * 100\%$$

The loading content (LC%) of the exenatide-loaded NPs was calculated using formula II:

$$LC\% = \frac{encapsulated\ exenatide}{weight\ of\ nanoparticles} * 100\%$$

Cell Studies

Cell Culture

Caco-2 and HT29 cells were cultivated separately in 21-cm^2 culture dishes using DMEM supplemented with 15% fetal bovine serum and 1% non-essential amino acids. Both cell types were placed in a cell culture incubator at 37°C, with 95% relative humidity and 5% CO_2. Prior to cytotoxicity and uptake assays, the cells were digested with 0.25% trypsin containing 0.05 mM ethylenediamine tetraacetic acid (EDTA) and then diluted with fresh DMEM to a density of $1*10^5$ cells /ml. For the cytotoxicity assays, the Caco-2 and HT-29 cell suspensions were individually seeded into 96-well plates (Corning, NY, USA) and incubated for 5 days; the HT-29 cells were incubated for another 2 days for the uptake studies. For the transport experiments, Caco-2 and HT29 cells were mixed at a ratio of 10:1 and seeded in Transwell® chambers consisting of a polycarbonate membrane with a 0.4-mm pore size and 0.33-cm^2 cell growth area (Corning) at a density of $3*10^4$ cells/well. The Transwell® chambers were placed into 24-well plates, and DMEM was added to both the Transwell® chambers and the 24-well plates. The cells were allowed to grow and differentiate for 21 days until use (5).

Cytotoxicity

The cytotoxicities of chitosan and CSK-chitosan were assessed using the MTT assay with Caco-2 cells and HT29 cells, respectively. In brief, the culture medium in the 96-well plates was discarded. The cells were then rinsed with PBS buffer and

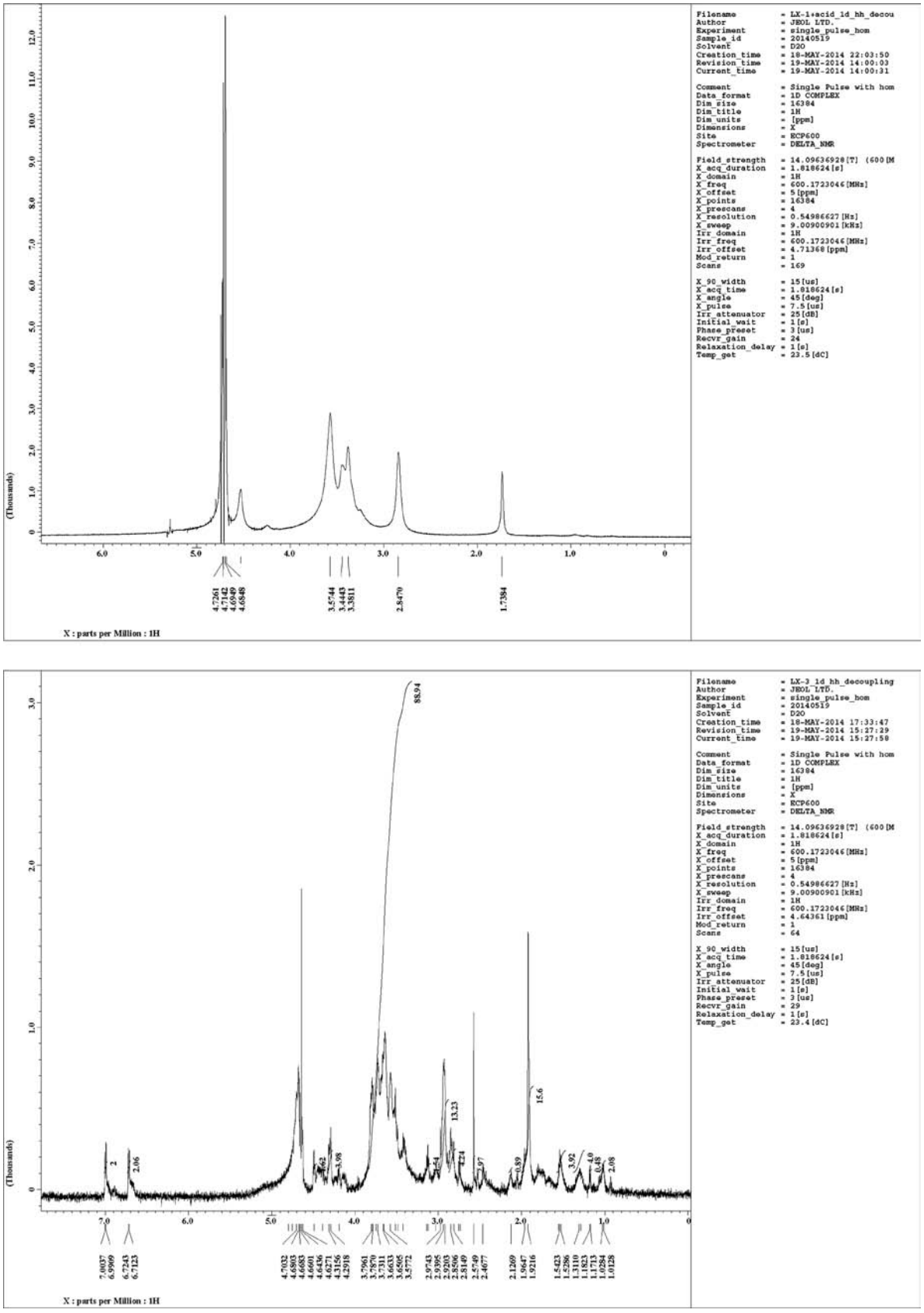

Fig. 1 (**a**) $_1$H NMR spectra of chitosan. (**b**) $_1$H NMR spectra of CSK-chitosan. (**c**) $_1$H NMR spectra of CSK peptide. The characteristic peaks at 7.11 and 6.81 ppm are the two protons of the benzene ring of tyrosine in the CSK peptide sequence.

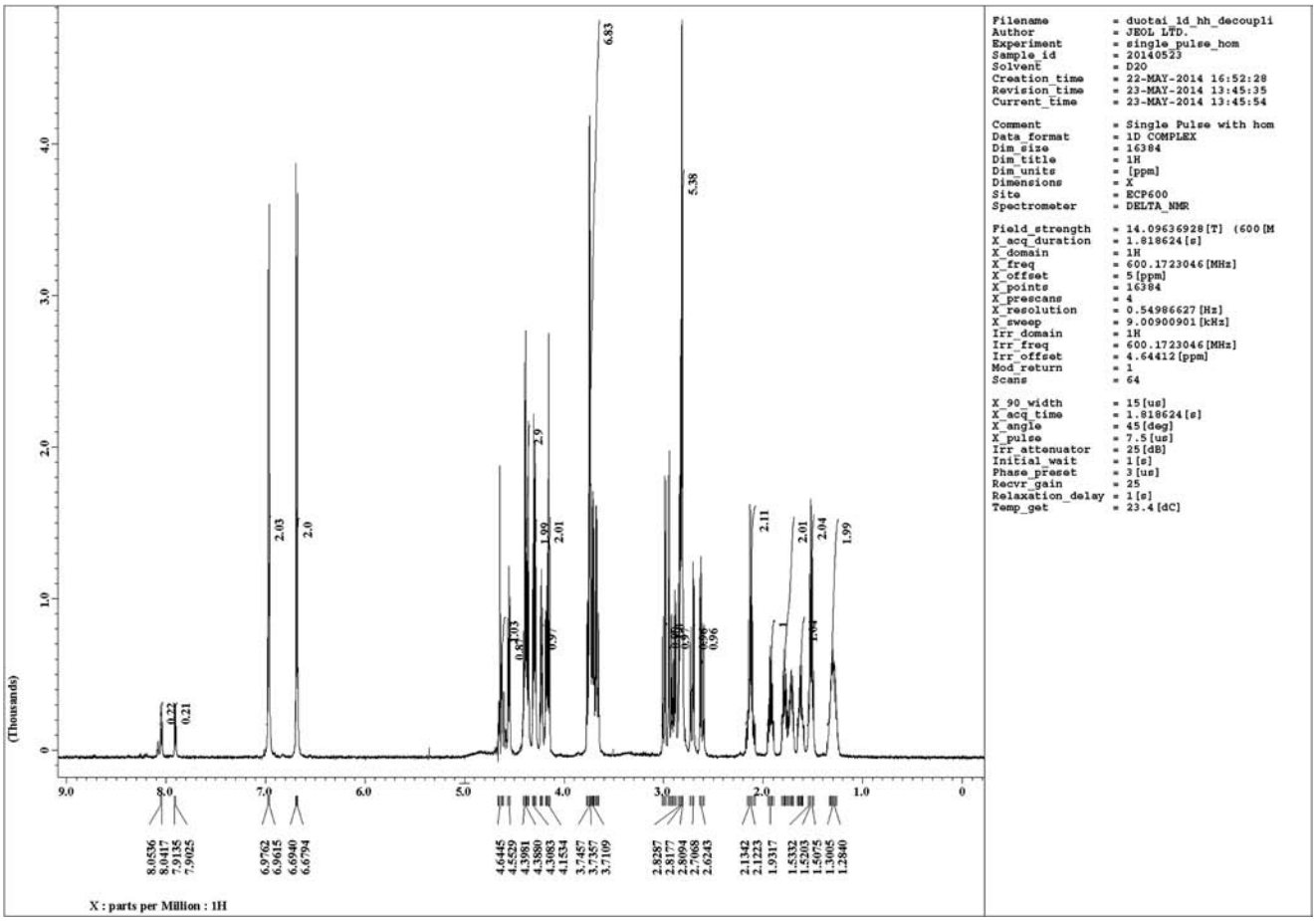

Fig. 1 (continued)

incubated with 100 µl of chitosan, chitosan-CSK (1:1) or chitosan-CSK (2:1) solution in PBS (pH 6.0) for 3 h (the concentrations of the chitosan and chitosan-CSK solutions were 0.125, 0.25, 0.37 and 0.5 mg/ml, at pH 6.0), and 100 µl of MTT solution (0.5 mg/ml in DMEM) was added. PBS buffer was used as a control for 100% cell viability. The assays were performed in triplicate for each sample (5).

Transport of Exenatide Through Caco-2 and HT29 Cell Monolayers

Caco-2 and HT29 cells were co-cultured and incubated for 19~21 days after culturing on the Transwell® inserts. Caco-2 can mimic epithelial cells, and HT29 cells mimic goblet cells by forming a mucus layer. The integrity of the monolayer was evaluated by measuring the transepithelial electric resistance (TEER) with a Millicell Electrical Resistance System (ERS) (Millipore Corp., Bedford, MA, USA). First, the media in the basolateral and apical chambers were exchanged with pre-warmed HBSS. The cells were then washed with HBSS three times and allowed to equilibrate at 37°C for 30 min. The cells were then incubated with 100 µl of chitosan FITC-exenatide NP or CSK-chitosan FITC-exenatide NP suspension (80 µg/ml of FITC-exenatide) and 100 µl of HBSS buffer at 37°C. At preset time points (0.5, 1, 2 and 3 h), 0.2 ml of the basolateral chamber sample was collected, and the same amount of pre-warmed HBSS was added. The amount of transported FITC-exenatide was measured with an enzyme-labeling measuring instrument, and the cumulative transfer of FITC-exenatide from the apical chamber was calculated. The transport of the three studied exenatide-loaded NPs was also examined in a non-mucus model to test the influence of the mucus layer and targeting by the CSK-chitosan NPs. The cells were pre-incubated with 10 mM acetylcysteine, which was used to remove the mucus secreted by the HT29 cells. The cells were agitated for 60 min before the ensuing experiment at 37°C (5).

Biodistribution Study

Cy-7-loaded NPs were used to investigate biodistribution using a near-infrared *in vivo* imaging system (FX Pro,

Table I Characterization of Nanoparticles

NPs	Size (nm)	Zeta potential (mV)	EE%	LC%
Chitosan NPs	181.5 ± 33.5	10.2 ± 2.9	70.2 ± 5.9	7.05 ± 0.58
CSK-chitosan NPs (1:1)	135.2 ± 18.5	6.3 ± 2.8	55.3 ± 7.9	5.87 ± 0.89
CSK-chitosan NPs (1:2)	142.3 ± 19.1	7.2 ± 1.5	57.6 ± 5.8	5.96 ± 0.75
CSK-chitosan FITC-exenatide NPs	156.2 ± 26.3	7.5 ± 2.7	49.6 ± 11.2	5.32 ± 0.53

EE%: entrapment efficiency; LC%: loading content

Bruker, USA). Mice were orally delivered 1.0 ml of Cy-7-loaded CSK-chitosan (1:1) after anesthetization with an i.p. injection of sodium pentobarbital at 10 mg/100 g body weight. At different time points, the anesthetized mice were placed into the chamber, and the fluorescence images and X-ray images were visualized using an *in vivo* imaging system.

Pharmacological Studies

In this study, db/db mice were used as a model of Type II diabetes (15). All experiments were performed according to the Guidelines for Animal Experiments, Jilin University. The glucose concentrations were measured with a glucose meter (ACCU-CHEK® Integra, Germany). Before oral administration of exenatide-loaded NPs, a $NaHCO_3$ solution (0.2 ml, 12.5 mg/ml) was intragastrically (i.g.) administered to neutralize the gastric acid (5). Diabetic mice were treated with the following: oral administration of chitosan exenatide NPs (30.0 μg/kg exenatide), CSK-chitosan (1:1) exenatide NPs (30.0 μg/kg exenatide), CSK-chitosan (1:2) exenatide NPs (30.0 μg/kg exenatide), exenatide solution (7.5 μg/kg exenatide) or physiological saline or an SC injection of exenatide solution (5.0 μg/kg). Blood samples were collected from the tail veins at different time intervals (0, 1, 2, 3, 4, 6, 8, 10 and 12 h), and the blood glucose was measured with a glucose meter.

Pharmacokinetics Study

In the pharmacokinetics study, male SD rats weighing 250 ± 20 g were used, and $NaHCO_3$ solution (0.5 ml, 12.5 mg/ml) was administered i.g. before oral administration of exenatide-loaded NPs. The SD rats were then treated with the following: oral administration of chitosan exenatide NPs (50.0 μg/kg exenatide), CSK-chitosan (1:1) exenatide NPs (50.0 μg/kg exenatide), CSK-chitosan (1:2) exenatide NPs (50.0 μg/kg exenatide) or exenatide solution (50.0 μg/kg exenatide) or an SC injection of exenatide solution (5.0 μg/kg exenatide). Blood samples (0.5 ml) were collected from the eye veins of the rats at

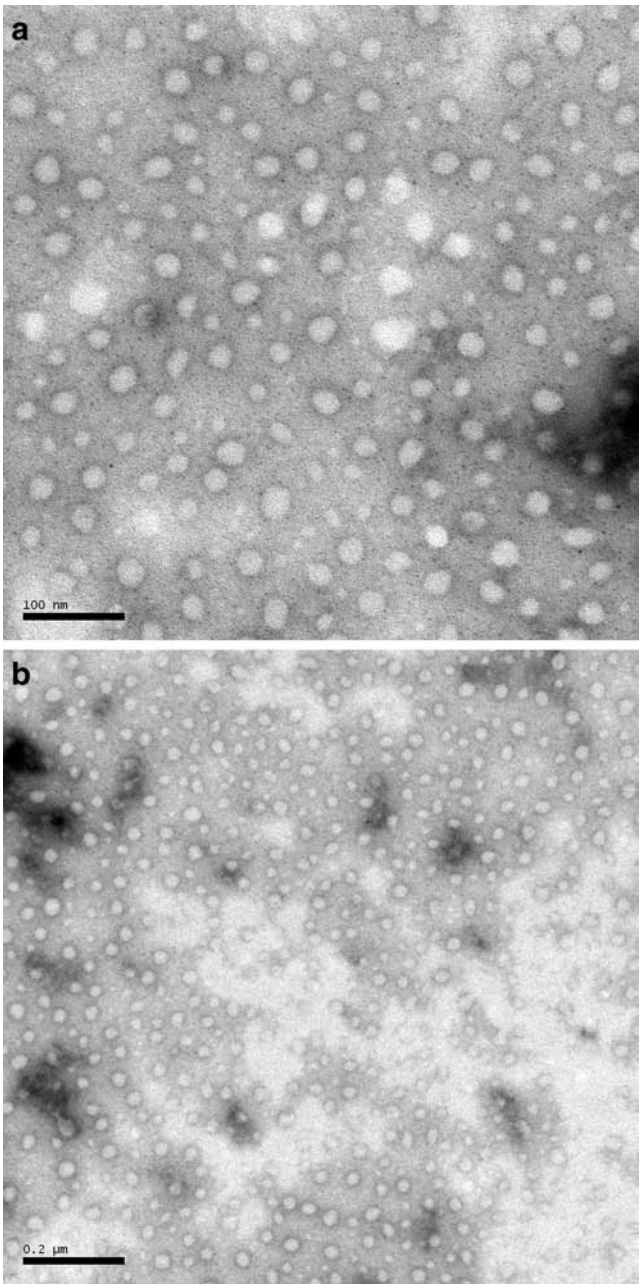

Fig. 2 (**a**) and (**b**) TEM micrographs of CSK-chitosan NPs.

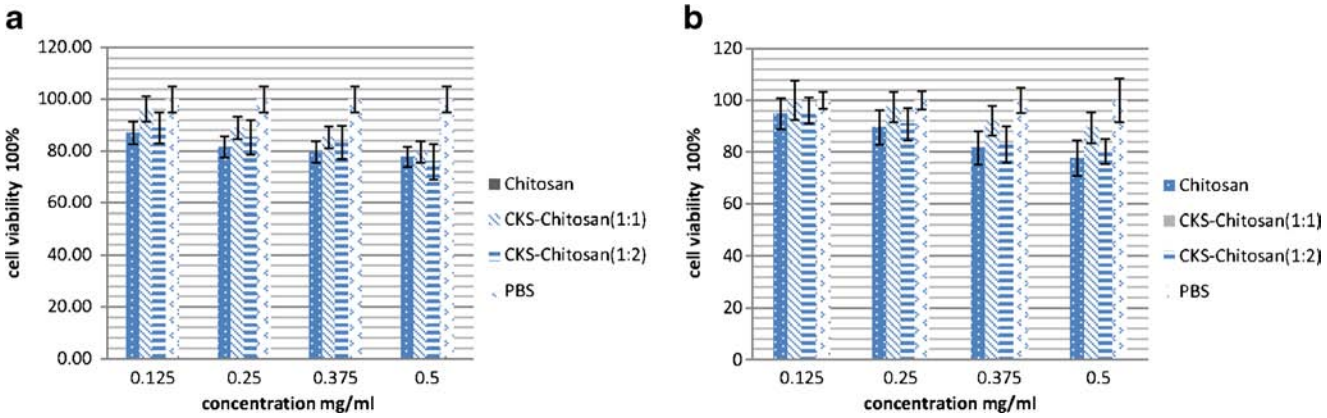

Fig. 3 (**a**) Influence of PBS, chitosan and CSK-chitosan on the viability of Caco-2 cells. (**b**) Influence of PBS, chitosan and CSK-chitosan on the viability of HT-29 cells (Mean ± SD, $n = 6$).

different time points (0, 0.5, 1, 2, 3, 4, 6, 8, 10 and 12 h). The relative bioavailability (BA%) of the exenatide-loaded NPs was calculated using formula III:

$$BA = \frac{AUC(oral) * Dose(SC)}{AUC(SC) * Dose(oral)} * 100\%$$

The AUC is the total area under the curve of the exenatide concentration in plasma *vs.* time. To analyze the concentration of exenatide, the serum samples obtained after centrifugation were tested using an Exenatide Fluorescent ELISA kit (Phoenix Pharmaceuticals, Inc., USA).

Statistical Analysis

All experiments were performed at least in triplicate. The data are presented as the means ± standard deviation (SD). Comparisons between two groups were analyzed using a two-tailed Student's *t*-test. A difference of $P < 0.05$ was considered statistically significant, and <0.01 was considered highly significant.

RESULTS AND DISCUSSION

Characterization of Synthesized Polymers

To synthesize CSK-chitosan, the N-amino group of chitosan was combined with the carboxyl group at the C-terminus of the CSK peptide via an amide linkage. The molar ratios of chitosan and CSK peptide were 6:1 and 3:1. The ^{1}H NMR spectra are shown in Fig. 1a, b and c. The characteristic peaks of CSK-chitosan are at 7.11 and 6.81 ppm and are attributable to the two protons of the benzene ring of tyrosine in the CSK peptide sequence (5). Because of the overlap of the glucose unit peaks of chitosan, the other proton peaks of CSK-chitosan, ranging from 0.8 to 4.6 ppm, were indistinguishable from those of chitosan.

Characteristics of NPs

The characteristics of exenatide-loaded and blank NPs (including chitosan exenatide NPs, CSK-chitosan exenatide NPs, chitosan FITC-exenatide NPs and CSK-chitosan FITC-exenatide NPs) are summarized in Table I. The TEM micrographs of the CSK-chitosan NPs are shown in Fig. 2a

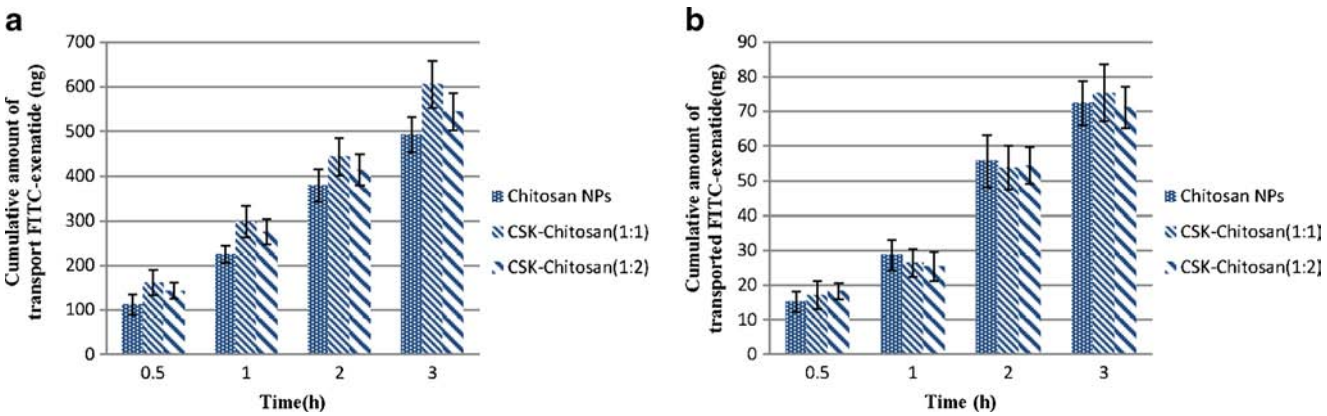

Fig. 4 (**a**) Transport of chitosan FITC-exenatide NPs and CSK-chitosan FITC-exenatide NPs across a co-incubated Caco-2/HT29 monolayer. (**b**) Transport of chitosan FITC-exenatide NPs and CSK-chitosan FITC-exenatide NPs across a co-incubated Caco-2/HT29 monolayer without mucus (Mean ± SD, $n = 6$).

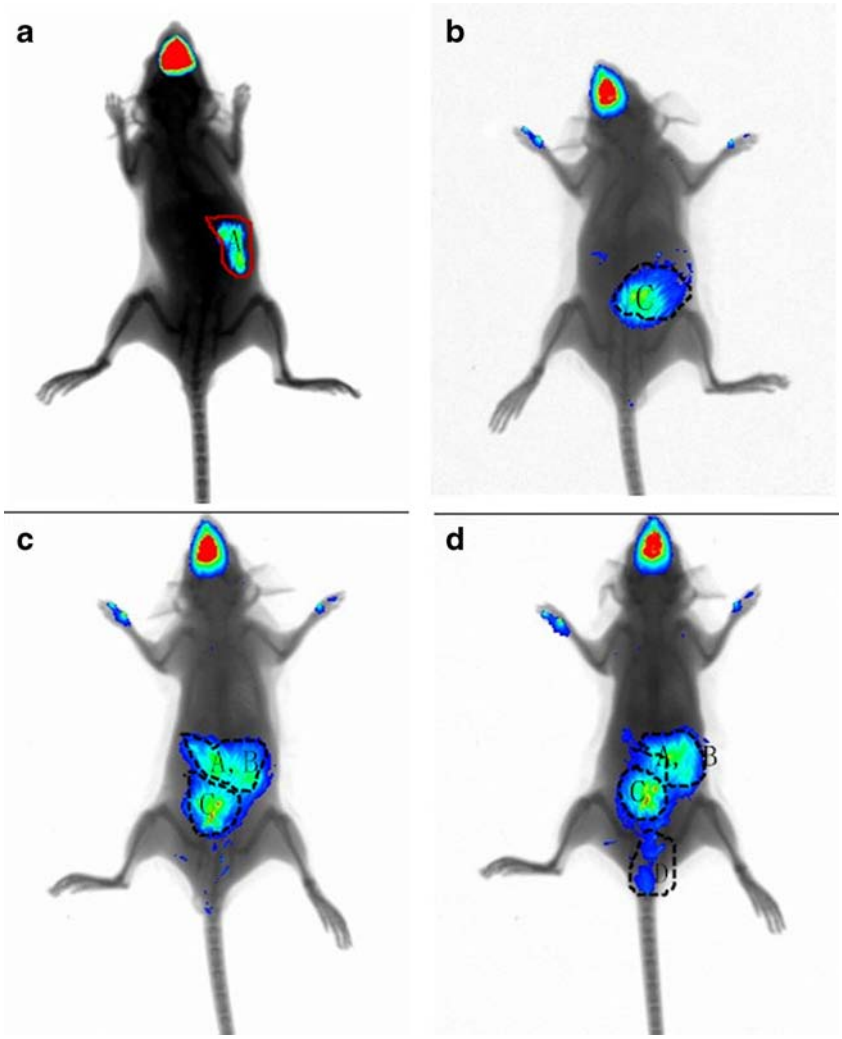

Fig. 5 *In vivo* fluorescence images of FITC-exenatide distribution after the administration of physiological Cy-7-loaded CSK-chitosan NPs at 0.5 h (**a**), 1 h (**b**), 2 h (**c**) and 4 h (**d**) after administration. A:Stomach;B: intestine;C: Liver;D: Bladder

and b. Both the chitosan NPs and CSK-chitosan NPs were uniformly sized spheres. Figure 2a shows obvious small black points that most likely represent $FeSO_2$. The addition of $FeSO_2$ enhances the encapsulation efficiency, as reported by Nguyen *et al.* (16). Table I shows that the drug-loaded chitosan NPs were larger and had a lower zeta potential than the NPs prepared with CSK-chitosan, which might result from the introduction of CSK. The CSK peptide has a molecular weight (MW) of 1,018 Da and is negatively charged. With the negatively charged CSK peptide, the electropositivity of chitosan was weakened and could bind to fewer negatively charged molecules. Therefore, the amount of TPP was lower in the CSK-chitosan NP formulation than in the chitosan NP formulation. The EE% and LC% were also lower for the CSK-chitosan NPs than the chitosan NPs.

Cytotoxicity of Polymers

To assess the safety of CSK-chitosan, the viability of Caco-2 cells and HT29 cells in the presence of this compound were tested separately in the MTT assay. Chitosan, CSK-chitosan

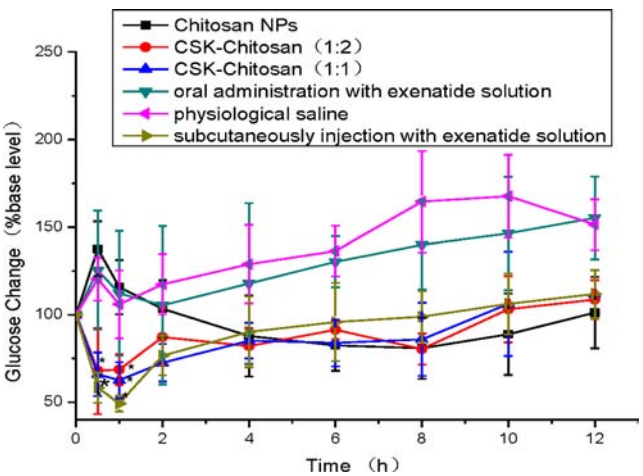

Fig. 6 Blood glucose levels in diabetic rats following the oral administration of chitosan NPs, CSK-chitosan (1:1) NPs, CSK-chitosan (1:2) NPs (30.0 μg/kg exenatide), exenatide solution (7.5 μg/kg exenatide), physiological saline and SC injection with exenatide solution (5.0 μg/kg) (Mean ± SD, $n = 6$). * Significant difference from SC exenatide solution ($P < 0.05$).

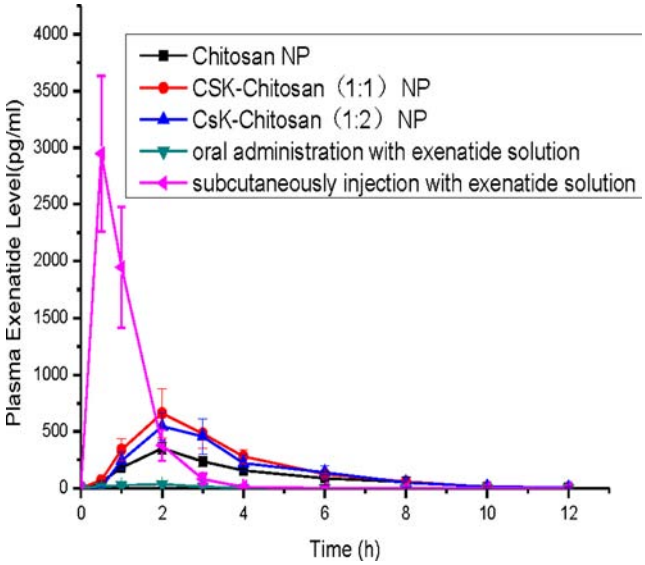

Fig. 7 Plasma exenatide level *vs.* time profiles. Plasma exenatide level in diabetic rats following the oral administration of chitosan NPs, CSK-chitosan (1:1) NPs, CSK-chitosan (1:2) NPs and exenatide solution (50 IU/kg), with the SC injection of exenatide solution (5.0 IU/kg) used as a positive control (Mean ± SD, $n = 6$).

(1:1) and CSK-chitosan (1:2) displayed lowcytotoxicity from 0.125 to 0.5 mg/ml for the Caco-2 and HT29 cells in the MTT assay. The influences of PBS, chitosan and CSK-chitosan on the viability of Caco-2 cells and HT29 cells are shown in Fig. 3a and b. The results demonstrated that modification with the CSK peptide decreased the cytotoxicity of chitosan. This phenomenon might be due to the negative charges of the CSK peptide masking the positive charges of chitosan. Furthermore, there was no significant difference between CSK-chitosan and PBS in terms of cellular viability, and these data suggest that CSK-chitosan is non-toxic to Caco-2 and HT29 cells.

Transport of Exenatide Through a Caco-2 and HT29 Cell Monolayer

Encapsulated exenatide must cross the intestinal epithelial cells for exenatide to be absorbed into the circulatory system. Therefore, a co-cultured cell model including Caco-2 cells, which are absorptive enterocyte-like cells, and HT29 cells, which produce mucus, was used to assess the transport of chitosan NPs. This co-culture model simulates the intestinal epithelium due to the existence of a mucus layer that is near the true value of the TEER of the intestinal epithelium (17). The co-cultured cell monolayers used in the experiment had TEER values within the range of 400–500 Ω. The accumulative transportation of FITC-exenatide in every NP is presented in Fig. 4a. The transport was time-dependent, and the amount of FITC-exenatide that permeated through the Caco-2/HT29 cell monolayer greatly increased with the addition of the CSK peptide at every time point. Moreover, the amount of FITC-exenatide that was transported across the membrane increased with the addition of the CSK peptide. Figure 4b shows that removal of the mucus did not affect the amount of FITC-exenatide transported. The amount of FITC-exenatide transported using modified and unmodified NPs was much higher in the co-culture system than in the non-mucus system at every time point. This is in agreement with the report of Kissel (18). However, in some other reports, the mucus layer acts as a diffusion barrier, and the reported observations are quite different from ours (19). However, in these reports, Caco-2 cells were used as a mucus-free model, and HT29 cells were used as a mucus-secreting cell model. The permeation behavior of HT29 cells was quite different compared with the Caco-2 cells. Because HT29 cells may not form tight junctions (TJs), as shown by the TEER measurement, the TEER of the co-culture model was lower than that of the Caco-2 model (data not shown). Therefore, the use of HT29 cells alone to imitate intestinal cells is not an effective model.

Biodistribution

In this study, Cy-7-loaded NPs were used to investigate the distribution of NPs because Cy-7 is soluble in water and because it carries cations when dissolved in water. Following the oral delivery of the Cy-7-loaded NPs, the biodistribution of the drug in mice was investigated using an *in vivo* imaging system (20,21), largely because using fluorescent material instead of radioactive material is much safer for the researcher.

Table II Pharmacokinetic Parameters of Exenatide in Diabetic rats after the Intragastric Administration (i.g.) of Chitosan NP, CSK-chitosan (1:1) NP, CSK-chitosan (1:2) NP, Exenatide Solution and SC Administration of INS Solution ($n = 6$)

	Chitosan NP (i.g.)	CSK-chitosan (1:1) NP (i.g.)	CSK-chitosan (1:2) NP (i.g.)	Exenatide solution (i.g.)	Exenatide solution (SC)
Dose (μg/kg)	50	50	50	50	5
C_{max} (pg/ml)	352.36 ± 51.16	662.63 ± 218.19	544.72 ± 117.815	33.68 ± 17.85	2,948.56 ± 685.32
T_{max} (h)	2	2	2	2	0.25
AUC (pg h/ml)	1,289.88	2,238.09	1,929.98	72.23	3,409.16
F_R%	3.78	6.56	5.66	0.21	100

C_{max}: maximum plasma concentration; T_{max}: time at which C_{max} is attained; FR: relative bioavailability

This study was the first time that an *in vivo* imaging system was utilized to evaluate the biodistribution of drug delivered orally. Figure 5 shows the whole-body fluorescence at 0.5 h (a), 1 h (b), 2 h (c) and 4 h (d) post-injection of Cy-7-loaded CSK-chitosan NPs. The fluorescence of Cy-7 expanded from the stomach to the intestine and then to liver and finally the bladder.

Pharmacological Effects

The pharmacological effects of chitosan exenatide NPs and CSK-chitosan exenatide NPs were evaluated in db/db mice after oral administration. As shown in Fig. 6, both CSK-chitosan (1:1) NPs and CSK-chitosan (1:2) NPs displayed comparatively high hypoglycemic effects, in contrast with exenatide solution, at 0.5 and 1.0 h after administration ($P<0.05$). Compared with chitosan NPs, no blood glucose increase from stress, which can occur after i.g. administration, was observed. The oral administration of exenatide solution or physiological saline did not lower the blood glucose levels, indicating poor oral absorption of the free form of exenatide in the small intestine. The oral administration of CSK-chitosan (1:1) NPs showed nearly the same effect as SC injection of the exenatide solution and due to the fact that the mechanism of action of exenatide does not result in severe hypoglycemic events (22). Exenatide is able to stimulate β-cells to release insulin when under hypoglycemic conditions, whereas the drug does not stimulate insulin secretion when the glucose concentration is within the normal range (23).

Pharmacokinetics Studies

The plasma exenatide concentration *vs.* time profiles and related PK parameters are shown in Fig. 7 and Table II, respectively. Exenatide was undetectable In the plasma of the group that received the exenatide solution orally. The group that received the drug SC showed the maximum plasma exenatide concentration at 0.5 h post-injection. However, oral administration of chitosan NPs, CSK-chitosan (1:1) NPs or CSK-chitosan (1:2) NPs resulted in maximum plasma concentration at 2 h post-administration. In this case, the AUC of CSK-chitosan (1:1) NPs was 2,238.09 ± 156.32 pg h/ml, and the relative bioavailability was 6.56%, 1.7-fold higher than that of the unmodified chitosan NPs.

Overall, the *in vivo* pharmacological and pharmacokinetic results were consistent with the *in vitro* cell studies. The relative bioavailability demonstrated that chitosan NPs and CSK-chitosan NPs can effectively prevent enzymatic exenatide degradation in the GIT and facilitate its absorption and thus systemic circulation.

CONCLUSIONS

We developed a formulation for goblet cell-targeting nanoparticles for the oral delivery of exenatide. The use of the CSK peptide as a targeting agent enhanced the transport of the drug across a co-cultured Caco-2 and HT29 cell membrane compared with unmodified NPs. After modifying chitosan with the CSK peptide, the hypoglycemic effect of CSK-chitosan NPs was significantly improved. The relative bioavailability of CSK-chitosan was improved to 1.7-fold higher than the unmodified form. The administered exenatide was absorbed, resulting in systemic circulation, and prolonged the hypoglycemic effect. These results indicate that CSK-chitosan effectively targets goblet cells and is a promising carrier for the oral delivery of peptides and proteins.

REFERENCES

1. Gedulin BR, Smith PA, Jodka CM, Chen K, Bhavsar S, Nielsen LL, *et al.* Pharmacokinetics and pharmacodynamics of exenatide following alternate routes of administration. Int J Pharm. 2008;356:231–8.
2. Eng J, Kleinman WA, Singh L, Singh G, Raufman JP. Isolation and characterization of exendin-4, an exendin-3 analogue, from Heloderma suspectum venom. Further evidence for an exendin receptor on dispersed acini from guinea pig pancreas. J Biol Chem. 1992;267:7402–5.
3. Goke R, Fehmann HC, Linn T, Schmidt H, Krause M, Eng J, *et al.* Exendin-4 is a high potency agonist and truncated exendin-(9–39)-amide an antagonist at the glucagon-like peptide 1-(7–36)-amide receptor of insulin-secreting beta-cells. J Biol Chem. 1993;268:19650–5.
4. Hamman JH, Enslin GM, Kotze AF. Oral delivery of peptide drugs: barriers and developments. BioDrugs. 2005;19:165–77.
5. Jin Y, Song Y, Zhu X, Zhou D, Chen C, Zhang Z, *et al.* Goblet cell-targeting nanoparticles for oral insulin delivery and the influence of mucus on insulin transport. Biomaterials. 2012;33:1573–82.
6. Felt O, Buri P, Gurny R. Chitosan: a unique polysaccharide for drug delivery. Drug Dev Ind Pharm. 1998;24:979–93.
7. Zhao J, Fan X, Zhang Q, Sun F, Li X, Xiong C, Zhang C, Fan H. Chitosan-plasmid DNA nanoparticles encoding small hairpin RNA targeting MMP-3 and −13 to inhibit the expression of dedifferentiation related genes in expanded chondrocytes. J Biomed Mater Res A. 2013.
8. Sonaje K, Lin K-J, Wey S-P, Lin C-K, Yeh T-H, Nguyen H-N, *et al.* Biodistribution, pharmacodynamics and pharmacokinetics of insulin analogues in a rat model: Oral delivery using pH-Responsive nanoparticles vs. subcutaneous injection. Biomaterials. 2010;31:6849–58.
9. Dash M, Chiellini F, Ottenbrite RM, Chiellini E. Chitosan—A versatile semi-synthetic polymer in biomedical applications. Prog Polym Sci. 2011;36:981–1014.
10. Shiraishi S, Imai T, Otagiri M. Controlled release of indomethacin by chitosan-polyelectrolyte complex: optimization and in vivo/in vitro evaluation. J Control Release. 1993;25:217–25.
11. Jin C-H, Chae SY, Son S, Kim TH, Um KA, Youn YS, *et al.* A new orally available glucagon-like peptide-1 receptor agonist, biotinylated exendin-4, displays improved hypoglycemic effects in db/db mice. J Control Release. 2009;133:172–7.

12. Roger E, Lagarce F, Garcion E, Benoit J-P. Biopharmaceutical parameters to consider in order to alter the fate of nanocarriers after oral delivery. Nanomedicine (London, U K). 2010;5:287–306.
13. Kang SK, Woo JH, Kim MK, Woo SS, Choi JH, Lee HG, *et al.* Identification of a peptide sequence that improves transport of macromolecules across the intestinal mucosal barrier targeting goblet cells. J Biotechnol. 2008;135:210–6.
14. Gupta V, Doshi N, Mitragotri S. Permeation of insulin, calcitonin and exenatide across Caco-2 monolayers: measurement using a rapid, 3-day system. PLoS One. 2013;8:e57136.
15. Wangand Q, Brubaker PL. Glucagon-like peptide-1 treatment delays the onset of diabetes in 8 week-old db/db mice. Diabetologia. 2002;45:1263–73.
16. Nguyen HN, Wey SP, Juang JH, Sonaje K, Ho YC, Chuang EY, *et al.* The glucose-lowering potential of exendin-4 orally delivered via a pH-sensitive nanoparticle vehicle and effects on subsequent insulin secretion in vivo. Biomaterials. 2011;32:2673–82.
17. Hilgendorf C, Spahn-Langguth H, Regardh CG, Lipka E, Amidon GL, Langguth P. Caco-2 versus Caco-2/HT29-MTX co-cultured cell lines: permeabilities via diffusion, inside- and outside-directed carrier-mediated transport. J Pharm Sci. 2000;89:63–75.
18. Behrens I, Pena AI, Alonso MJ, Kissel T. Comparative uptake studies of bioadhesive and non-bioadhesive nanoparticles in human intestinal cell lines and rats: the effect of mucus on particle adsorption and transport. Pharm Res. 2002;19:1185–93.
19. Schipper NG, Varum KM, Stenberg P, Ocklind G, Lennernas H, Artursson P. Chitosans as absorption enhancers of poorly absorbable drugs. 3: influence of mucus on absorption enhancement. Eur J Pharm Sci. 1999;8:335–43.
20. Deliolanisand NC, Ntziachristos V. Fluorescence molecular tomography of brain tumors in mice. Cold Spring Harb Protocol. 2013;2013:438–43.
21. Xiang Y, Liang L, Wang X, Wang J, Zhang X, Zhang Q. Chloride channel-mediated brain glioma targeting of chlorotoxin-modified doxorubicine-loaded liposomes. J Control Release. 2011;152:402–10.
22. Gallwitz B. The evolving place of incretin-based therapies in type 2 diabetes. Pediatr Nephrol. 2010;25:1207–17.
23. Nielsen LL, Young AA, Parkes DG. Pharmacology of exenatide (synthetic exendin-4): a potential therapeutic for improved glycemic control of type 2 diabetes. Regul Pept. 2004;117:77–88.